

Phase-field simulations of faceted Ge/Si-crystal arrays, merging into a suspended film

Marco Salvalaglio^{a,1,*}, Roberto Bergamaschini^a, Rainer Backofen^b, Axel Voigt^b, Francesco Montalenti^a, Leo Miglio^a

^a*L-NESS and Department of Materials Science, Università di Milano-Bicocca via R. Cozzi 55, I-20126, Milano, Italy*

^b*Institut für Wissenschaftliches Rechnen, Technische Universität Dresden, D-01062, Dresden, Germany*

Abstract

We simulate the morphological evolution of Ge microcrystals, grown out-of-equilibrium on deeply-patterned Si substrates, as resulting from surface diffusion driven by the tendency toward the minimization of the surface energy. In particular, we report three-dimensional phase-field simulations accounting for the realistic surface energy anisotropy of Ge/Si crystals. In [M. Salvalaglio et al., ACS Appl. Mater Interfaces 7, 19219 (2015)] it has been shown both by experiments and simulations that annealing of closely spaced crystals leads to a coalescence process with the formation of a suspended film. However, this was explained only by considering an isotropic surface energy. Here, we extend such a study by showing first the morphological changes of faceted isolated crystals. Then, the evolution of dense arrays is considered, describing their coalescence along with the evolution of facets. Combined with the previous results without anisotropy in the surface energy, this work allows us to confirm and assess the key features of the coalescence process.

Keywords: Heteroepitaxy, Surface diffusion, Phase field, Germanium, Surface energy

*Corresponding author.

Email address: marco.salvalaglio@tu-dresden.de (Marco Salvalaglio)

¹Present address: Institut für Wissenschaftliches Rechnen, Technische Universität Dresden, D-01062, Dresden, Germany.

1. Introduction

Heteroepitaxy of semiconductors is widely exploited to improve the performances of opto- and micro-electronic devices. A well-known example is represented by $\text{Si}_{1-x}\text{Ge}_x$ films grown on Si(001) substrates, as they are a key for the heterogeneous integration of electronic components in the Si-based technology [1]. Indeed, the Ge/Si system, characterized by both lattice (4.2%) and thermal (130%) misfit, can be considered a prototype for the investigation of more complex configurations involving other materials. In close-to-equilibrium conditions, i.e. high temperatures and low deposition fluxes, the growth of Ge films on Si is initially characterized by the formation of self-assembled three-dimensional (3D) islands, following the so-called Stranski-Krastanov growth modality [2, 3]. At later stages, the insertion of linear defects, i.e. dislocations, is eventually observed [4]. For deposition rates (and/or temperatures) high (low) enough to substantially reduce the surface diffusion length, i.e. in out-of-equilibrium conditions, the formation of planar films is achieved from the very beginning, relaxing the lattice strain by the insertion of misfit dislocations [5]. Still, two main technological problems are encountered. First, the misfit segments of dislocations at the Ge/Si interface terminate at the film surface by threading arms, which are very detrimental for the performances of devices. Second, thick enough films generate wafer warping and cracks, due to the different thermal expansion coefficients of Si and Ge [6].

Recently, vertical 3D Ge (or $\text{Si}_{1-x}\text{Ge}_x$) crystals on deeply patterned Si substrates have been demonstrated at the micron scale by Low Energy Plasma Enhanced Chemical Vapor Deposition (LEPECVD) [7]. In contrast to the growth on planar substrates, separated crystals were obtained with large height-to-base aspect ratios and peculiar 3D morphologies characterized by a complex faceting [8]. This was achieved thanks to the out-of-equilibrium conditions ensured by LEPECVD. In particular, the growth kinetics was mainly determined by both the orientation-dependent incorporation rate and the mutual shielding of the incoming material flux [7, 8]. Such vertical structures were proven to be of very

high crystalline quality [7]. Moreover, thanks to their high aspect-ratio, they permit to confine dislocations threading arms in the lower part of the crystals [9] and fully relax thermal strain [7].

In Ref. [10] we investigated the evolution of these vertical Ge/Si heterostructures induced by annealing. The coalescence of closely spaced crystals was reported, providing a viable path for the formation of high-quality suspended networks, with promising properties for the heterogeneous integration of semiconductors. This mechanism was explained by taking into account the thermally-activated surface diffusion [11, 12], driven by the tendency toward the minimization of the surface energy only. Indeed, at variance with standard heteroepitaxy [13], the elastic energy contribution is typically negligible in Ge/Si vertical crystals thanks to the peculiar elastic and plastic relaxation mechanisms [7, 14]. Moreover, volumetric contributions promoting the alloying of different materials during post-growth annealing are expected to affect only a small region of a few monolayers at the Ge/Si interface [13], not influencing the evolution of the Ge surface. Dedicated simulations were performed exploiting a 3D Phase-Field (PF) model [15]. Such an approach was selected to conveniently tackle the evolution of complex geometries, also in the presence of major topological changes. For the sake of simplicity, however, only isotropic surface energy was there considered.

Thus, the evolution of Ge microstructures was qualitatively described by neglecting any dependence of the surface energy on the local orientation $\hat{\mathbf{n}}$ [10], although crystals are known to exhibit preferential faceting which results from anisotropic surface energy densities $\gamma(\hat{\mathbf{n}})$ [16, 17]. In general, once $\gamma(\hat{\mathbf{n}})$ values are known, the equilibrium crystal shapes (ECS) can be obtained by means of the so-called Wulff construction [18, 19]. However, more advanced tools are required to describe the changes in the faceting of crystals during the evolution towards the equilibrium [20]. Despite the initial faceting of Ge microcrystals is determined by the growth kinetics [8], the surface-energy dependence on $\hat{\mathbf{n}}$ is expected to become important for high-temperature treatments, as close-to-equilibrium conditions are achieved. Indeed, experiments clearly show changes

in the faceting during post-growth annealing processing. Actually, new facets characteristic of the ECS appear, which are absent in the as grown profile [10].

The PF framework deals with the description of surface diffusion evolution
65 in the presence of an anisotropic $\gamma(\hat{\mathbf{n}})$ [15]. This holds true also in the strong anisotropy regime, i.e. when sharp corners appear in the ECS and a proper energy regularization should be adopted as the evolution equations become ill-defined [21]. Moreover, such an approach has been demonstrated to tackle
70 that the diffuse-interface approach allow for a general description of material processing also accounting for the growth with anisotropic velocities (see for instance Refs. [23, 24]). Therefore, it also represents a promising tool for the investigation of competitive mechanisms involving both surface diffusion and growth dynamics.

75 At variance from Ref. [10], in this work we aim to provide a more realistic description of the crystals coalescence by explicitly accounting for the anisotropy in the surface energy, responsible for the faceting in the thermodynamic regime of annealing. This provides a better match to the experimental evidence and permits a deeper understanding of the mechanisms behind coalescence. In particular, we first discuss the definition of a continuous $\gamma(\hat{\mathbf{n}})$ function, obtained
80 by interpolating the values of the known preferential orientations of Ge crystals reported in literature [16]. PF simulations of surface diffusion accounting for this definition of $\gamma(\hat{\mathbf{n}})$ are then performed to assess the morphological evolution of isolated microcrystals during annealing. Closely spaced crystals are finally
85 considered in order to describe their coalescence along with the facets evolution, and the role of the surface anisotropy is discussed.

2. Phase-field model

In order to describe the morphological evolution by surface diffusion for 3D crystals, we adopted a continuum description based on the so-called phase-field
90 (PF) model [15]. An auxiliary function $\varphi(\mathbf{x})$ is used as an order parameter de-

scribing the solid phase, $\varphi = 1$, and the vacuum phase, $\varphi = 0$, with a continuum variation in between. A suitable choice for φ is given by

$$\varphi(\mathbf{x}) = \frac{1}{2} \left[1 - \tanh \left(\frac{3d(\mathbf{x})}{\epsilon} \right) \right], \quad (1)$$

with ϵ the interface thickness and $d(\mathbf{x})$ the signed distance from the surface of the solid phase, namely the $\varphi \sim 0.5$ isosurface. The evolution based on thermodynamic driving forces requires to define the free energy F as a function of φ . Since the crystals are fully-relaxed from the mechanical point of view (by both plastic and elastic relaxation mechanisms), and intermixing effects can be neglected [7], only surface energy should be considered. According to Ref. [21], the energy functional is

$$F[\varphi] = \int_V \gamma(\hat{\mathbf{n}}) \left(\frac{\epsilon}{2} |\nabla\varphi|^2 + \frac{1}{\epsilon} B(\varphi) \right) d\mathbf{x} + \int_V \frac{\beta}{2\epsilon} \kappa(\varphi)^2 d\mathbf{x}. \quad (2)$$

The first integral is the Ginzburg-Landau functional, with $B(\varphi) = 18\varphi^2(1-\varphi)^2$, $\gamma(\hat{\mathbf{n}})$ the surface energy density and $\hat{\mathbf{n}} = -\nabla\varphi/|\nabla\varphi|$ the outer-pointing surface normal. The second integral is the regularization required for strongly anisotropic systems, namely the Willmore regularization [21], which correspond to an edge/corner energy term [25]. $\kappa(\varphi) = -\epsilon\nabla^2\varphi + (1/\epsilon)B'(\varphi)$ is the approximation of the curvature in the PF approach. This regularization produces a rounding of the corners controlled by the β parameter. The surface diffusion mechanism [11, 12] is then derived as an evolution law for φ [15] as

$$\frac{\partial\varphi}{\partial t} = \nabla \cdot (M(\varphi)\nabla\mu), \quad (3)$$

with $M(\varphi) = 2M_0B(\varphi)/\epsilon$ the mobility function restricted to the surface, with M_0 as a scaling factor, and μ the chemical potential. The latter is defined by [21]

$$g(\varphi)\mu = \delta F/\delta\varphi = -\epsilon\nabla \cdot [\gamma(\hat{\mathbf{n}})\nabla\varphi] + \frac{1}{\epsilon}\gamma(\hat{\mathbf{n}})B'(\varphi) - \epsilon\nabla \cdot [|\nabla\varphi|^2\nabla_{\nabla\varphi}\gamma(\hat{\mathbf{n}})] + \beta \left(-\nabla^2\kappa + \frac{1}{\epsilon^2}B''(\varphi)\kappa \right) \quad (4)$$

with $\nabla_{\nabla\varphi}$ the gradient along the direction of $\nabla\varphi$ and $g(\varphi) = 30\varphi^2(1-\varphi)^2$ a stabilizing function included to improve the convergence of the present PF

model to the surface diffusion in the sharp-interface limit, recovered for $\epsilon \rightarrow 0$ [26, 27]. In the following we will consider time expressed in arbitrary units. For consistency with the Ge/Si vertical heterostructures reported in the literature, e.g. in Refs. [7, 8, 10], the unit of length is scaled in μm .

The numerical integration of the evolution law for φ is obtained by solving the system of the partial differential equations for $\partial\varphi/\partial t$, $g(\varphi)\mu$ and κ . A semi-implicit integration scheme similar to the one reported in Ref. [22] is considered, with numerical stability improved by following the approach proposed in Ref. [28]. The implementation of such a framework has been performed within the AMDiS Finite Element Method toolbox [29, 30], and solved by both direct and iterative solvers. In order to optimize the required calculations, a non-uniform space discretization has been adopted with refined mesh at the interface, where surface diffusion evolution is active.

3. Anisotropic surface energy

When considering the anisotropy of the surface energy, the data available in the literature typically consist of a discrete set of γ values for the preferential orientations. From these data, one can calculate the expected ECS in agreement with the Wulff construction [18]. In Fig. 1a, such a shape is calculated using the Wulffmaker software [31], accounting for the main families of facets for Ge, i.e. $\{100\}$, $\{113\}$, $\{111\}$ and $\{110\}$, and the corresponding surface energy values reported in Ref. [16].

The PF approach described in Sect. 2, however, requires a continuous $\gamma(\hat{\mathbf{n}})$ function with values for each orientation. The description of the anisotropic surface energy that we adopt here is based on the general expression of $\gamma(\hat{\mathbf{n}})$ introduced in Ref. [22], i.e.

$$\gamma(\hat{\mathbf{n}}) = \gamma_0 \left(1 - \sum_{i=1}^N \alpha_i (\hat{\mathbf{n}} \cdot \hat{\mathbf{m}}_i)^{w_i} \Theta(\hat{\mathbf{n}} \cdot \hat{\mathbf{m}}_i) \right), \quad (5)$$

where N is the total number of the energy minima in $\gamma(\hat{\mathbf{n}})$ along the directions $\hat{\mathbf{m}}_i$ with depth α_i . The w_i parameters control the width of the minima, i.e. the

140 range of the orientations $\hat{\mathbf{n}}$ around $\hat{\mathbf{m}}_i$ where $\gamma(\hat{\mathbf{n}})$ is lower than γ_0 . For large enough w_i values, we have $\gamma(\hat{\mathbf{m}}_i) = \gamma_0(1 - \alpha_i)$. Θ is the Heaviside step function.

The surface energy of real Ge crystals is reproduced by selecting $\hat{\mathbf{m}}_i$ and α_i in order to match the orientations of the minima and the surface energy values reported in the literature [16]. In particular, we focus our attention on the main
 145 preferential orientations, corresponding to $\{100\}$, $\{113\}$, $\{111\}$ and $\{110\}$ facets as in Fig. 1a. The energy of the facets with normal along $\langle 100 \rangle$ directions is considered as a reference, assuming $\alpha_{\langle 100 \rangle} = 0.15$. The α_i coefficients are then obtained by

$$\alpha_i = 1 - \left(\frac{\gamma_i}{\gamma_{\langle 100 \rangle}} \right) (1 - \alpha_{\langle 100 \rangle}), \quad (6)$$

where i indicates one of the aforementioned families of facets and γ_i is the corresponding surface energy value reported in Ref. [16]. Notice that γ_0 is not present
 150 in Eq. 6 as it does not affect the ratio between different minima. Therefore it can be used as a scaling factor in order to match the desired magnitude of the surface energy. For the sake of simplicity we set $\gamma_0 = 1$. The w_i parameter has been selected equal to 100 for minima along $\langle 113 \rangle$ directions and to 50 for the
 155 other minima to ensure no superposition of the different contributions in the sum of Eq. (5) for each $\hat{\mathbf{m}}_i$ [22].

The $\gamma(\hat{\mathbf{n}})$ resulting from such a procedure, with α_i values from Eq. (6), is shown in Fig. 1b. This construction of the surface energy density accounts for every possible orientation of the crystal and not only for the ones correspond-
 160 ing to surface energy minima. In principle, this allows for a fine tuning of $\gamma(\hat{\mathbf{n}})$ including also the connections between facets. However, these orientations are affected by local features of the crystals such as vicinal surfaces and step bunching, which are generally unknown and difficult to be addressed. With this respect, the formulation for the $\gamma(\hat{\mathbf{n}})$ function of Eq. 5 (as shown in Fig. 1b)
 165 represents a convenient fit of a continuous function passing through the known energy minima.

The equilibrium configuration given by the $\gamma(\hat{\mathbf{n}})$ function shown in Fig. 1b is obtained by the PF model of surface diffusion described in Sect. 2, starting from

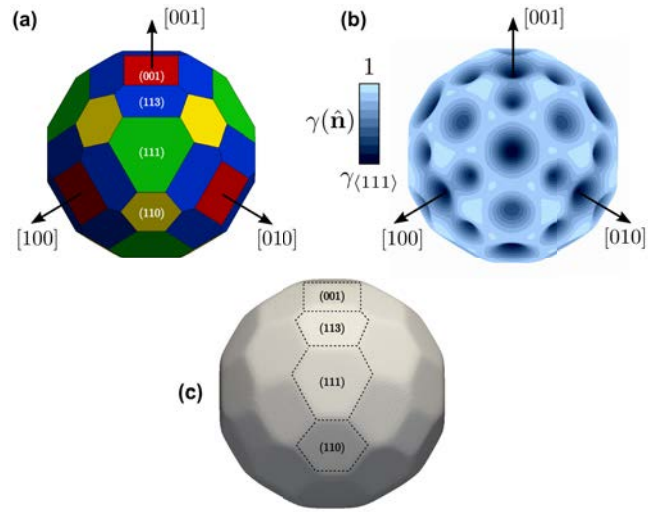


Figure 1: Surface energy density and equilibrium shape. (a) Equilibrium crystal shape bounded only by $\{100\}$, $\{113\}$, $\{111\}$ and $\{110\}$ facets. Their extensions is set according to the surface energy density values in Ref. [16] (computed by Wulffmaker [31]) (b) $\hat{\mathbf{n}}\gamma(\hat{\mathbf{n}})$ plot of the continuous surface energy function obtained by tuning Eq. (5) with the minima of the surface energy as in panel (a). The color map shows the values of $\gamma(\hat{\mathbf{n}})$. (c) Equilibrium configuration obtained by a PF simulation of surface diffusion, in the presence of the anisotropic $\gamma(\hat{\mathbf{n}})$. Dashed lines illustrate the outline of the resulting facets.

a sphere. The initial profile is set by considering Eq. (1) with $\epsilon = 0.05$ and a
 signed distance defined by $d(\mathbf{x}) = |\mathbf{x}| - R$ with R the radius of the sphere, set to
 170 1 in the present simulation. Hereafter the reported surface profiles correspond
 to the 0.5 iso-surface of $\varphi(\mathbf{x})$. The regularization parameter β is arbitrarily
 set to 0.003 to ensure small rounding at corners and edges. The differences in
 $\gamma(\hat{\mathbf{n}})$ on the surface of the sphere induce a material flux following the gradient
 175 of the chemical potential, as described by Eq. (3), and lead to the equilibrium
 configuration. The final shape shows a faceting of the surface resembling the
 morphology in Fig. 1a but it also includes the intermediate orientations with
 respect to the preferential ones. The regularization term in Eq. (2) avoids the
 presence of sharp edges and corners producing rounded connections between
 180 facets [21, 22]. This leads to a slightly different shape than the one in Fig. 1a
 and the outlines of the facets are not sharply defined. However, the equilibrium
 configuration keeps all the main features obtained by the Wulff construction, as
 also shown by the dashed lines in Fig. 1c.

It is worth mentioning here that the evolution described by the PF model
 185 provides a real kinetic pathway towards the equilibrium crystal shape starting
 from any initial configuration. Moreover, the description of a realistic surface
 energy is included. However, the present model does not account for the possi-
 ble energy barriers for the diffusion among different facets (thus assuming full
 activation of the diffusion processes) whose description requires a dedicated de-
 190 velopment of the considered PF framework, out of the purposes of the present
 work. The assumption considered in the model revealed to be effective in de-
 scribing the main features of the evolution by an a-posteriori comparison with
 the evidences in Ref. [10].

4. Results and Discussion

195 As assessed in Ref. [10], the evolution in time of the 3D Ge microstructures
 with large (height-to-base) aspect-ratios and isotropic surface energy, is mainly
 characterized by a rounding of the crystals, leading to the lowering of the aspect-

ratios. This is the key enabling feature for the coalescence process occurring in closely spaced crystals. When accounting for the anisotropic surface energy, as shown in Fig. 1c, facets are obtained and this may significantly affect the global rounding and the lateral expansion. Actually, some investigations have been reported in the literature describing the evolution by surface diffusion of elongated structures, such as simple rectangles or parallelepipeds, in the presence of surface faceting. Results have been obtained, for instance, by a fully-faceted approach in 2D [20] or within the PF model dealing with the 3D evolution [22]. According to these works, an enlargement of the elongated structures is still obtained also in the presence of faceting. This suggests that this feature will be also present when explicitly considering the anisotropy of $\gamma(\hat{\mathbf{n}})$ in our system of interest.

In order to investigate this behavior in the specific case of 3D Ge microcrystals, we focus on the typical experimental structures introduced in Ref. [7]. They are obtained by deposition of Ge, up to a thickness of $8 \mu\text{m}$, on $2 \times 2 \mu\text{m}^2$ wide, $8 \mu\text{m}$ tall Si pillars. In particular, we consider a realistic initial profile closely resembling the morphology of the experimental shape obtained at a growth temperature of $\sim 500 \text{ }^\circ\text{C}$ [7, 8] (see $t = 0$ in Fig. 2). The Si pillar below the Ge crystal is modeled as a simple cylinder where the mobility vanishes, i.e. $M_0 \sim 0$ [10]. This is justified by the very low mobility of Si compared to the Ge one [32] at the typical processing temperatures, up to $\sim 800 \text{ }^\circ\text{C}$ during annealing. The presence of a small amount of Ge on the sidewalls of the Si pillars is also considered, in agreement with the experimental evidence.

The evolution by surface diffusion of such a structure with the $\gamma(\hat{\mathbf{n}})$ defined in Sect. 3, is shown in Fig. 2, where $\epsilon = 0.2$. The color map shows the local $\gamma(\hat{\mathbf{n}})$ values, highlighting the presence of the facets where a uniform color is obtained at almost constant $\hat{\mathbf{n}}$. Moreover, rounded connections between facets, with high values of $\gamma(\hat{\mathbf{n}})$, are obtained as imposed by the regularization in Eq. (2) [21]. In the first stages, the original faceting resulting from the kinetic growth is modified by surface diffusion. Indeed, the pyramid bounded by $\{113\}$ facets at the top of the crystal in the initial configuration, evolves into a truncated pyramid with

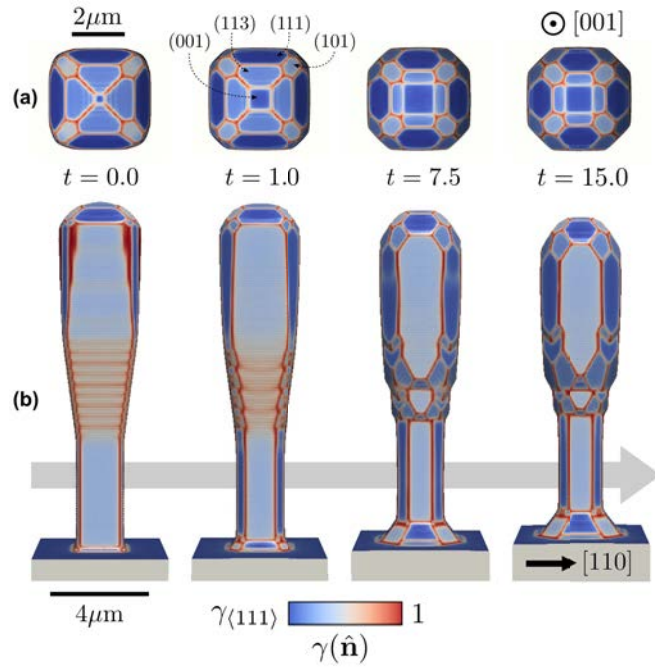


Figure 2: Evolution by surface diffusion of an isolated crystal. The initial geometry is set to closely resemble the experimental one obtained at a growth temperature of $\sim 500^\circ\text{C}$ in Refs. [7, 8]. (a) Top and (b) lateral view of four representative stages are reported. The color map shows the $\gamma(\hat{\mathbf{n}})$ values. Dashed arrows mark the families of facets. Time is expressed in arbitrary units.

the clear appearance of the (001) facet, as expected from the equilibrium crystal
 shape (see Fig. 1). This feature has been directly observed in the experiments
 in Ref. [10] and cannot be reproduced by the evolution with isotropic surface
 energy. Moreover, the facets which are stable according to the surface energy,
 and already present in the initial configuration, are preserved. Faceted sidewalls
 appear as imposed by the choice of $\gamma(\hat{\mathbf{n}})$ with also the formation of (± 100) and
 (0 ± 10) facets at the vertical edges. At the bottom of the Ge crystals, where the
 initial profile shows unstable orientations, a complex faceting is formed involving
 several different facets, providing the average slope required to match the size
 of the Si pillar with the Ge crystal on top. A transfer of the material around
 the Si pedestal towards the planar substrate is also observed, until exposing the
 Si. Indeed, faceting at the bottom of the whole structure is observed and the
 height of the planar region around the structure increases. As can be noticed
 from Fig. 2, comparing the first stages with the morphology at $t = 15$, the
 global evolution leads to a lowering of the crystal which results also slightly
 enlarged. In agreement with the evidence reported in Ref. [10], when considering
 closely spaced structures separated by a few tens of nanometers, this behavior
 would produce the filling of the gap between the crystals. So that coalescence
 occurs and the dynamics varies significantly with respect to the isolated crystals
 discussed so far.

The more complex evolution of crystal arrays is here investigated by focusing
 on the same initial geometry used for the simulations of Fig. 2, in order to
 reproduce an evolution as close as possible to the real systems. In particular, the
 initial profile consists of crystals aligned along the $[110]$ and the $[\bar{1}10]$ directions
 with a periodicity equal to $4 \mu\text{m}$. The resulting gap between crystals is \sim
 $0.4 \mu\text{m}$. Periodic boundary conditions are considered for the lateral sidewalls
 of the simulation cell. The evolution for such a system is illustrated in Fig. 3,
 where representative stages of the PF simulations are shown. Color map shows
 the local $\gamma(\hat{\mathbf{n}})$ values as in Fig. 2. In the first stages of the evolution, crystals
 are not affected by the neighbors and the morphological changes are the same
 as discussed for isolated crystals ($t = 1.0$, as in Fig. 2). Then, coalescence

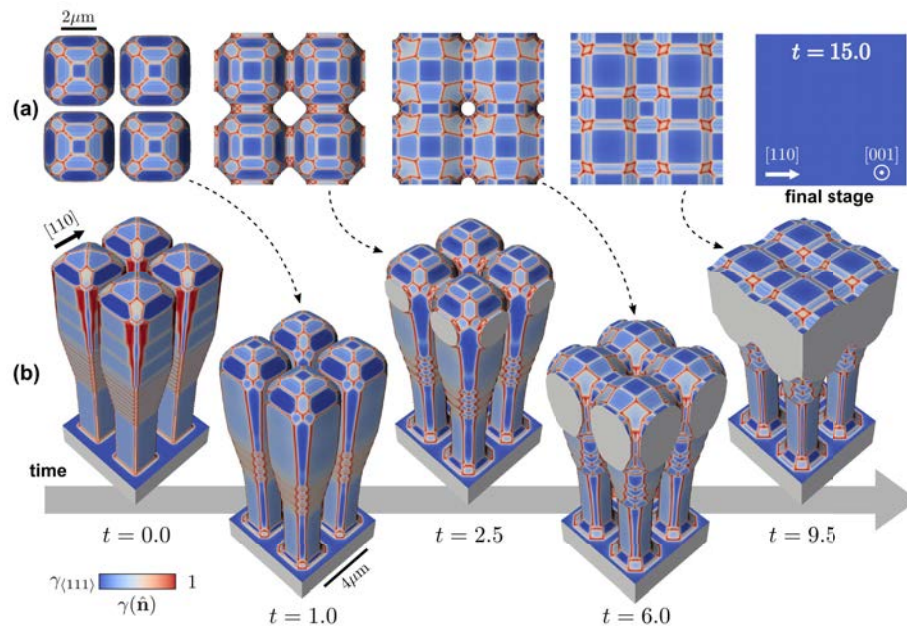


Figure 3: Surface diffusion evolution by the PF simulation of closely spaced crystals. (a) Top view of the crystals at representative stages of the evolution. The last top view (upper right-hand corner) shows the final stage corresponding to the complete flattening of the suspended film. (b) Perspective view of the three-dimensional evolution. Time is expressed in arbitrary units.

260 of crystals along $[110]$ and $[\bar{1}10]$ directions is obtained. Bridges are formed in
 between (as shown for $t = 2.5$). These regions act as sinks collecting material
 from the surroundings as can be appreciated by comparing the extension of
 the merging at $t = 2.5$ and $t = 6.0$. This produces a global lowering of the
 upper portion of the crystal with the disappearance of large $\{111\}$ facets at
 265 the top, favoring the extension of $\{113\}$ facets. Also $\{110\}$ facets, which may
 extend due to the free surface between bridges (see $t = 6.0$), grow larger up to
 the closure of the holes while (001) facets are formed on top of the coalesced
 regions. At later stages the complete closure of the holes is achieved, resulting
 in a continuous surface with a faceted profile as shown at $t = 9.5$. During this
 270 stage, new (001) facets are formed when holes are filled while the other flat
 regions extend. Moreover, the extension of $\{113\}$ and $\{110\}$ facets is gradually
 reduced. Eventually, the suspended film flattens and a single (001) surface is
 obtained on top of the structure as the final stage ($t = 15$), shown by means of
 the top view at the upper right-hand corner of Fig. 3.

275 Further insights on the coalescence process can be extracted by looking at
 the values of the free energy in time, namely $F(t)$, with F defined by Eq. (2).
 In Fig. 4 we show the $F(t)$ values, normalized with respect to the surface energy
 of the initial configuration (at $t = 0$). Two abrupt changes of the slope can be
 easily recognized and correspond to the topological changes of the structure, i.e.
 280 the coalescence of the crystals and the filling of the holes. In the other stages,
 an almost smooth decrease of the energy is observed. The end of the evolution
 is achieved when $F(t)$ reaches a constant value. All these features are general as
 they are observed also with isotropic $\gamma(\hat{\mathbf{n}})$. Furthermore, they are not affected
 by the specific choice of the surface energy.

285 From the results obtained so far we can conclude that the explicit description
 of the anisotropic surface energy allows for a more detailed description of the
 whole evolution by surface diffusion. Moreover, it does not lead to differences in
 the general mechanism of coalescence, as can be easily inferred by a comparison
 of the simulations provided here with the evolution in the presence of isotropic
 290 surface energy in Ref. [10]. However, it is clear that the presence of facets

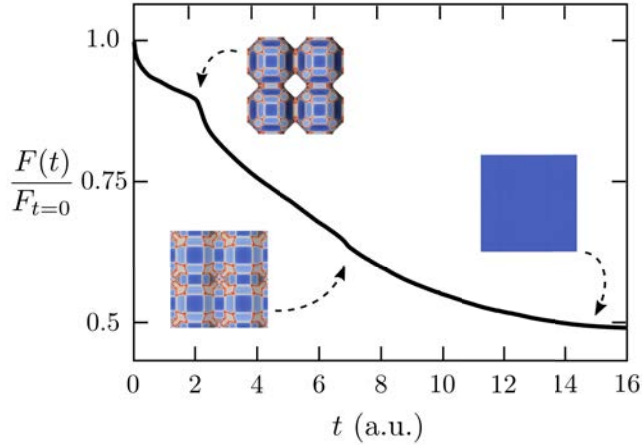


Figure 4: Surface energy decrease during the evolution by surface diffusion for the simulation of crystal coalescence reported in Fig. 3. Insets show top view of the evolving morphology at representative steps.

imposes some constraints on the whole shape. For instance, in contrast to the rounding obtained with isotropic $\gamma(\hat{\mathbf{n}})$, faceted sidewalls are obtained here. As far as the coalescence occurs when sidewalls get in contact, this is expected to play a role.

295 In order to clarify this point we consider a simplified system made of crystals with a cylindrical shape and a height-to-base aspect ratio resembling the experimental systems of Ref. [7]. Alignment along [100] and [010] directions is considered with a gap between crystals of $0.5 \mu\text{m}$. Then, two different $\gamma(\hat{\mathbf{n}})$ functions are selected (including, however, some preferential orientations for Ge
300 crystals), yielding different faceting at the sidewalls. In particular, $\gamma_1(\hat{\mathbf{n}})$ is set with $\hat{\mathbf{m}}_i$ along all $\langle 111 \rangle$ and $\langle 100 \rangle$ directions while $\gamma_2(\hat{\mathbf{n}})$ is set with $\hat{\mathbf{m}}_i$ along the directions of the same family but only with a positive component along the [001] direction. For both these definitions we select $\alpha_i = 0.1$ and $w_i = 30$. This way, sidewalls are forced to exhibit (± 100) and (0 ± 10) facets when considering $\gamma_1(\hat{\mathbf{n}})$
305 while they result in a rounded profile with $\gamma_2(\hat{\mathbf{n}})$. A difference in the onset of coalescence is observed when considering $\gamma_1(\hat{\mathbf{n}})$ or $\gamma_2(\hat{\mathbf{n}})$, as illustrated in Fig. 5. The elapsed time of the simulations is the same for both the panels of Fig. 5 but,

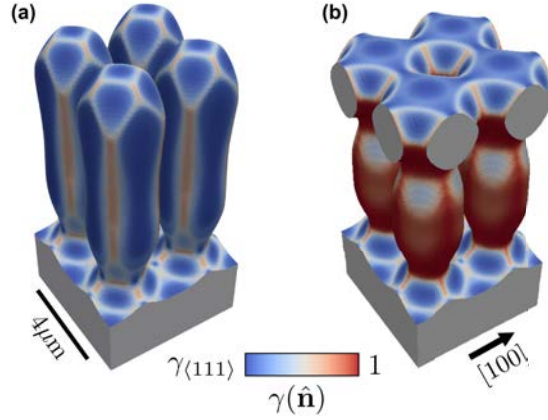


Figure 5: Coalescence occurrence with different (simplified) surface energy anisotropies. The initial condition and the elapsed time is the same for both the simulations where two different $\gamma(\hat{\mathbf{n}})$ definitions are considered: (a) $\gamma_1(\hat{\mathbf{n}})$ with $\hat{\mathbf{m}}_i$ along $\langle 111 \rangle$ and $\langle 100 \rangle$ directions and (b) $\gamma_2(\hat{\mathbf{n}})$ with minima along only the $\langle 111 \rangle$ and $\langle 100 \rangle$ directions with positive component along the $[001]$ direction. Color map shows the $\gamma(\hat{\mathbf{n}})$ values.

despite coalescence already occurred when considering $\gamma_2(\hat{\mathbf{n}})$, separated crystals are still present with $\gamma_1(\hat{\mathbf{n}})$. Therefore, when straight facets are enforced at the
 310 sidewalls, the enlargement leading to the coalescence is actually slowed down. However, in agreement with the simulations of Fig. 3, the merging of crystals is expected to occur at later stages also with $\gamma_2(\hat{\mathbf{n}})$.

5. Conclusions

In this work, we have theoretically investigated the morphological evolution
 315 of vertical Ge/Si heterostructures triggered by the surface diffusion mechanism in the presence of a realistic description of Ge surface-energy anisotropy [16], providing a direct application of the general formulation introduced in Ref. [22]. Simulations by means of a PF model of surface diffusion were exploited to describe the 3D evolution of the Ge crystals, involving the thermodynamic faceting
 320 of the initial profile and the global morphological change of the whole micro-crystals.

This investigation provided a detailed description of the expected evolution when promoting surface diffusion mechanism, e.g. when increasing the temperature during annealing experiments [10] or deposition [33]. In particular, the evolution of isolated Ge/Si structures was shown, together with the description of the coalescence of closely spaced crystals. If the general evidence of such an evolution have been presented first in Ref. [10] by neglecting anisotropy, the present work allowed us to clarify important additional details of the evolution during annealing and to strengthen the previous theoretical analysis. In Ref. [10] lateral enlargement of the crystals during annealing was identified as the key mechanism leading to coalescence. Here, we assessed this conclusion by showing that anisotropic surface energy does not change qualitatively the process. Indeed, the presence of faceting does not fully inhibit the lateral enlargement, which determines the contact between crystals and in turn the merging of crystals. However, we also showed that tackling preferential faceting is crucial if a close comparison with experiments is desired. The presence of surface facets is found to generally affect the time scale of the morphological evolution and also prevents the formation of unrealistic rounded surfaces. Moreover, some features predicted by our simulations nicely reproduce fine details of the annealing experiments of Ref. [10] as, for instance, the appearance of a defined (001) facet by the annealing of initial profile with a pyramid bounded by {113} facets at the top of the structures. This correspondence further confirms that the evolution of vertical Ge crystals obtained by annealing experiments is mainly determined by the activation of the surface diffusion driven by tendency toward the minimization of the surface energy.

References

- [1] D. J. P, Si/SiGe heterostructures: from material and physics to devices and circuits, *Semiconductor Science and Technology* 19 (10) (2004) R75.
- [2] Y. Mo, D. Savage, B. Swartzentruber, M. Lagally, Kinetic Pathway in

- 350 Stranski-Krastanov Growth of Ge on Si(001), *Physical Review Letters*
65 (8) (1990) 1020–1023. doi:10.1103/PhysRevLett.65.1020.
- [3] G. Medeiros-Ribeiro, A. M. Bratkovski, T. I. Kamins, D. A. A. Ohlberg,
R. S. Williams, Shape Transition of Germanium Nanocrystals on a Silicon
(001) Surface from Pyramids to Domes, *Science* 279 (1998) 353–355. doi:
355 10.1126/science.279.5349.353.
- [4] A. Marzegalli, V. A. Zinovyev, F. Montalenti, A. Rastelli, M. Stoffel,
T. Merdzhanova, O. G. Schmidt, L. Miglio, Critical Shape and Size for
Dislocation Nucleation in SiGe Islands on Si(001), *Physical Review Letters*
99 (2007) 235505–235508. doi:10.1103/PhysRevLett.99.235505.
- 360 [5] E. A. Fitzgerald, Dislocations in strained-layer epitaxy: theory, experiment,
and applications, *Materials Science Reports* 7 (3) (1991) 87–140. doi:
10.1016/0920-2307(91)90006-9.
- [6] D. J. Dunstan, Strain and strain relaxation in semiconductors, *J.*
Mater. Sci.-Mater. Electron. 8 (6) (1997) 337–375. doi:10.1023/A:
365 1018547625106.
- [7] C. V. Claudiu, H. von Känel, F. Isa, R. Bergamaschini, A. Marzegalli,
D. Chrastina, G. Isella, E. Müller, P. Niedermann, L. Miglio, Scaling
Hetero-Epitaxy from Layers to Three-Dimensional Crystals, *Science* 335
(2012) 1330–1334. doi:10.1126/science.1217666.
- 370 [8] R. Bergamaschini, F. Isa, C. V. Falub, P. Niedermann, E. Müller, G. Isella,
von Känel H, L. Miglio, Self-aligned Ge and SiGe three-dimensional epitaxy
on dense Si pillar arrays, *Surf. Sci. Rep.* 68 (2013) 390–417. doi:10.1016/
j.surfrep.2013.10.002.
- [9] A. Marzegalli, F. Isa, H. Groiss, E. Müller, C. V. Falub, A. G. Taboada,
375 P. Niedermann, G. Isella, F. Schäffler, F. Montalenti, H. von Känel,
L. Miglio, Unexpected dominance of vertical dislocations in high-misfit

Ge/Si(001) films and their elimination by deep substrate patterning, *Adv. Mater.* 25 (2013) 4408–4412. doi:10.1002/adma.201300550.

- [10] M. Salvalaglio, R. Bergamaschini, F. Isa, A. Scaccabarozzi, G. Isella,
380 R. Backofen, A. Voigt, F. Montalenti, G. Capellini, T. Schroeder, H. von
Känel, L. Miglio, Engineered Coalescence by Annealing 3D Ge Microstruc-
tures into High-Quality Suspended Layers on Si, *ACS Applied Materials &
Interfaces* 7 (34) (2015) 19219–19225. doi:10.1021/acsami.5b05054.
- [11] W. W. Mullins, Theory of Thermal Grooving, *J. Appl. Phys.* 28 (1957)
385 333–339. doi:10.1063/1.1722742.
- [12] W. W. Mullins, Flattening of a nearly plane solid surface due to capillarity,
Journal of Applied Physics 30 (1) (1959) 77–83. doi:10.1063/1.1734979.
- [13] R. Bergamaschini, M. Salvalaglio, R. Backofen, A. Voigt, A. Montalenti,
Continuum modeling of semiconducto heteroepitaxy: an applied perspec-
390 tive, *Advanced in Physics: X* In press. doi:10.1080/23746149.2016.
1181986.
- [14] M. Salvalaglio, F. Montalenti, Fine control of plastic and elastic relax-
ation in Ge/Si vertical heterostructures, *J. Appl. Phys.* 116 (2014) 104306–
104314. doi:10.1063/1.4895486.
- 395 [15] B. Li, J. Lowengrub, A. Voigt, Geometric Evolution Laws for Thin Crys-
talline Films: Modeling and Numerics, *Commun. Comput. Phys.* 6 (2009)
433–482.
- [16] Z. Gai, W. S. Yang, R. G. Zhao, T. Sakurai, Macroscopic and nanoscale
faceting of germanium surfaces, *Phys. Rev. B* 59 (1999) 15230–15239. doi:
400 10.1103/PhysRevB.59.15230.
- [17] A. A. Stekolnikov, F. Bechstedt, Shape of free and constrained group-IV
crystallites: Influence of surface energies, *Phys. Rev. B* 72 (2005) 125326.
doi:10.1103/PhysRevB.72.125326.

- [18] G. Wulff, *Zeitschrift für Kristallographie und Mineralogie* 34 (1901) 449–
405 530.
- [19] C. Herring, Some Theorems on the Free Energies of Crystal Surfaces, *Physical Review* 82 (1) (1951) 87–93. doi:10.1103/PhysRev.82.87.
- [20] W. C. Carter, A. Roosen, J. W. Cahn, J. Taylor, Shape evolution by surface
diffusion and surface attachment limited kinetics on completely faceted
410 surfaces, *Acta Metallurgica et Materialia* 43 (12) (1995) 4309–4323. doi:
10.1016/0956-7151(95)00134-H.
- [21] S. Torabi, J. Lowengrub, A. Voigt, S. Wise, J. Lowengrub, A. Voigt, A new
phase-field model for strongly anisotropic systems, *Proceedings of the Royal
Society A* 465 (2105) (2009) 1337–1359. doi:10.1098/rspa.2008.0385.
- 415 [22] M. Salvalaglio, R. Backofen, R. Bergamaschini, F. Montalenti, A. Voigt,
Faceting of Equilibrium and Metastable Nanostructures: A Phase-Field
Model of Surface Diffusion Tackling Realistic Shapes, *Cryst. Growth Des.*
15 (2015) 2787–2794. doi:10.1021/acs.cgd.5b00165.
- [23] G. Russo, P. Smereka, A Level-Set Method for the Evolution of Faceted
420 Crystals, *SIAM Journal on Scientific Computing* 21 (6) (2000) 2073–2095.
doi:10.1137/S1064827599351921.
- [24] L. K. Aagesen, M. E. Coltrin, J. Han, K. Thornton, Phase-field simulations
of GaN growth by selective area epitaxy from complex mask geometries,
Journal of Applied Physics 117 (2015) 194302. doi:10.1063/1.4921053.
- 425 [25] B. J. Spencer, Asymptotic solutions for the equilibrium crystal shape with
small corner energy regularization., *Physical review. E, Statistical, nonlinear,
and soft matter physics* 69 (2004) 011603. doi:10.1103/PhysRevE.
69.011603.
- [26] A. Rätz, A. Ribalta, A. Voigt, Surface evolution of elastically stressed films
430 under deposition by a diffuse interface model, *Journal of Computational
Physics* 214 (2006) 187–208. doi:10.1016/j.jcp.2005.09.013.

- [27] C. Gugenberger, R. Spatschek, K. Kassner, Comparison of phase-field models for surface diffusion, *Physical Review E* 78 (2008) 016703–016719. doi:10.1103/PhysRevE.78.016703.
- 435 [28] F. Chen, J. Shen, Efficient Energy Stable Schemes with Spectral Discretization in Space for Anisotropic Cahn-Hilliard Systems, *Communications in Computational Physics* 13 (5) (2012) 1189–1208. doi:10.4208/cicp.101111.110512a.
- [29] S. Vey, A. Voigt, AMDiS: adaptive multidimensional simulations, *Comput. Visual. Sci.* 10 (2006) 57–67. doi:10.1007/s00791-006-0048-3.
- 440 [30] T. Witkowski, S. Ling, S. Praetorius, A. Voigt, Software concepts and numerical algorithms for a scalable adaptive parallel finite element method, *Advances in Computational Mathematics* 41 (2015) 1145–1177. doi:10.1007/s10444-015-9405-4.
- 445 [31] R. V. Zucker, D. Chatain, U. Dahmen, S. Hagge, W. C. Carter, New software tools for the calculation and display of isolated and attached interfacial-energy minimizing particle shapes, *Journal of Materials Science* 47 (24) (2012) 8290–8302. doi:10.1007/s10853-012-6739-x.
- [32] L. Huang, F. Liu, G.-H. Lu, X. G. Gong, Surface Mobility Difference between Si and Ge and Its Effect on Growth of SiGe Alloy Films and Islands, *Phys. Rev. Lett.* 96 (2006) 016103. doi:10.1103/PhysRevLett.96.016103.
- 450 [33] R. Bergamaschini, M. Salvalaglio, A. Scaccabarozzi, F. Isa, V. F. Claudiu, I. Giovanni, von K Temperature-controlled coalescence during the growth of Ge crystals on deeply patterned Si substrates, *Journal of Crystal Growth* 440 (2016) 86 – 95. doi:10.1016/j.jcrysgro.2016.01.035.
- 455